



Highly efficient synthesis of chromeno[2,3-*b*]pyridine using Graphene-Oxide/*N*¹,*N*³-bis (pyridin-2-ylmethyl)propane-1,3-diamine-Copper nanocomposites as a novel catalyst

Zahra Karamshahi¹ | Ramin Ghorbani-Vaghei¹ | Hassan Keypour² | Mohammad Taher Rezaei²

¹Department of Organic Chemistry,
Faculty of Chemistry, Bu-Ali Sina
University, Box 65174, Hamedan, PO, Iran

²Department of Inorganic Chemistry,
Faculty of Chemistry, Bu-Ali Sina
University, Hamedan, Iran

Correspondence

Ramin Ghorbani-Vaghei, Department of
Organic Chemistry, Faculty of Chemistry,
Bu-Ali Sina University. PO Box 65174,
Hamedan, Iran.
Email: rgvaghei@yahoo.com

Recent studies about innovations in GO/N-Ligand-Cu Nano-Composites have been done. Graphene-Oxide is improved with *N*¹,*N*³-bis (pyridin-2-ylmethyl)propane-1,3-diamine and after that is matched with copper (Cu). The chemical composition and the structure of the catalyst were analyzed by TGA/DTG, EDX, XRD, FT-IR, TEM, and SEM. The results demonstrated that GO/N-Ligand-Cu was able to catalyze the chromeno[2,3-*b*]pyridine compounds to obtain high yields in short reaction time. The results of the present work are hoped to assist the growth of a new class of heterogeneous catalysts as the high-function candidate for industrial applications.

KEY WORDS

1,3-diamine, Chromeno[2,3-*b*]pyridine, graphene oxide, multi-component reactions, nanocomposites

1 | INTRODUCTION

Regarding the significant features of green chemistry, it is the catalysis which has been connected to the synthesis of chemical products and has also been regarded as an important tool in developing cleaner chemical processing. In this sense, developing new catalysts which have advantages like: lower input energies, higher selectivity, and decreasing toxic agents during the synthesis of certain chemicals can be considered as the main function of catalytic science. Moreover, it results in implementing simpler processes needed for and required by the green chemistry.^[1]

Amongst disparate carbon materials, graphene with two-dimensional structure due to its high specific surface area, unique electrical conductivity, self-assembly behavior, and mechanical flexibility has attracted widespread attention.^[2] The 21st century witnessed the arrival of a new material known as Graphene which attained wider attention after a work by Geim and his colleagues.^[3,4] It is on the GO Nano-Sheets that the oxygen functional

groups—i.e. hydroxyl group, epoxy, and carboxylic acid—have been applied in order to alter/transform graphene surface practicability.^[5,6]

It is worth mentioning that the chemical and mechanical properties of graphene and its derivatives – i.e. the oxidized graphene—would significantly affect producing novel materials in different scientific fields.^[1]

In this sense, a wide variety of methods have been organized in order to functionalize graphene i.e. carboxylic acid group esterification responses,^[7,8] the nucleophilic ring-opening reaction of epoxy group,^[9] isocyanate cure, etc.^[10]

When practical groups are present on the GO, superficial structures would be constructed in such a way that it will be capable of being utilized as an absorbent.^[11] In this regard, the ornamentation of inherent properties of graphene with metal nanoparticles (NPs) would result in their excellent adjustment to be applied for a wide variety of uses i.e. catalyst, energy generation, and storage, optoelectronics, and sensors.^[12,13]

During the last few years, much efforts have been dedicated to synthesize libraries of small heterocyclic molecules due to their great amount of structural variety and broad function as healing agents.^[14] In this study, the detection of central structures has this potential and not suffering from obvious overutilization is one of the chief challenges for the medicinal business in its quest for rich resources of recent molecular entities.^[15,16]

Heterocyclic compounds have a chief part in devising new classes of medicinally significant structural entities.^[17] Chromenopyridines are bonded with heterocyclic compounds that show a variety of biological happenings: antibacterial, antiproliferative (cytotoxic activity against the human solid tumor HT-29 cell lines), cancer chemopreventive, antirheumatic, antihistaminic, antimyopic and antiasthmatic.^[18,19] These scaffolds usually consist of a rigid ring hetero-system with specially defined orientation of different functionalities for aim diagnosis^[20] Multicomponent reactions (MCRs) are constantly effective sources and environmentally suitable and consequently greener in comparison to multistage reactions. Multicomponent reactions (MCRs) are greatly effective approaches to attain the prompt gathering of complex products, mainly progressive C-C and C-heteroatom bond-forming reactions in the field of heterocycles and healthy productions.^[19] We have chosen the most appropriate approach for preparing chromeno[2,3-*b*]pyridine compounds, those founded on multicomponent reactions (MCRs) (Scheme 1).

2 | EXPERIMENTAL

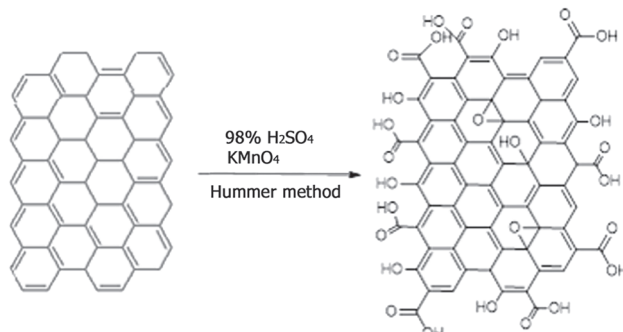
2.1 | Materials and methods

All commercial materials were purchased from Merck and Fluka companies, and used without further purifications. ¹H NMR and ¹³C NMR spectra were recorded on Bruker BioSpin GmbH 250 MHz FT NMR spectrometers, America. Fourier transform infrared (FT-IR) spectra were recorded on a Shimadzu 435-U-04 FT spectrophotometer, Columbia, Maryland from KBr tablets. Melting points were measured on a BUCHI, Gilroy, California 510 apparatus in open capillary tubes. Scanning electron

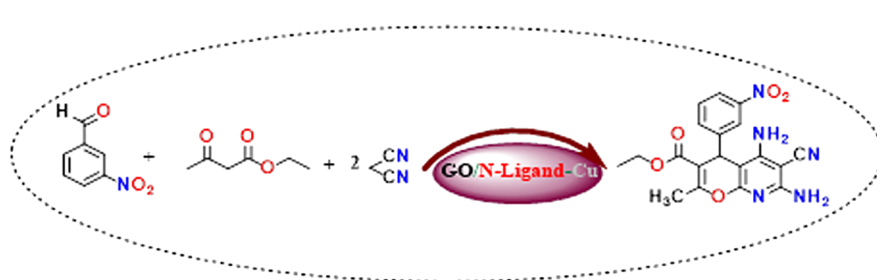
microscopy (SEM), Germany was performed on EM3200 instrument operated at 30 kV accelerating voltage. The structure of the new LDHs@Propyl-ANDSA was characterized using XRD, IR, SEM, EDX and TGA analysis. Energy dispersive X-ray (EDX), Nederland and Scanning electron microscopy (SEM) analysis of the prepared catalyst was fulfilled on a FESEM-SIGM (Germany) instrument. Thermo-gravimetric analysis (TGA) was accomplished on a DUPONT 951 TA, Texas City (America) Instruments. Transmission electron microscopy (TEM), Germany was performed with a Zeiss-EM10C-100 KV.^[21]

2.2 | Preparation of GO

Initially, natural graphite powder (2 g) was added into a 250 ml flask having 46 ml H₂SO₄ (98%) and it was stirred for 30 min. Then, NaNO₃ (1 g) was added to the mixture and stirred forcefully to prevent agglomeration. Subsequently, 6 g KMnO₄ and 20 ml H₂O₂ solution (30%) was progressively added into the flask and then cooled by putting in an ice bath. The blend was stirred for 45 min, then HCl (1 mol L⁻¹) was used to wash the resulting suspension and it was gathered by centrifugation (Scheme 2).^[22]



SCHM E 2 Schematic structure of graphene oxide (GO)

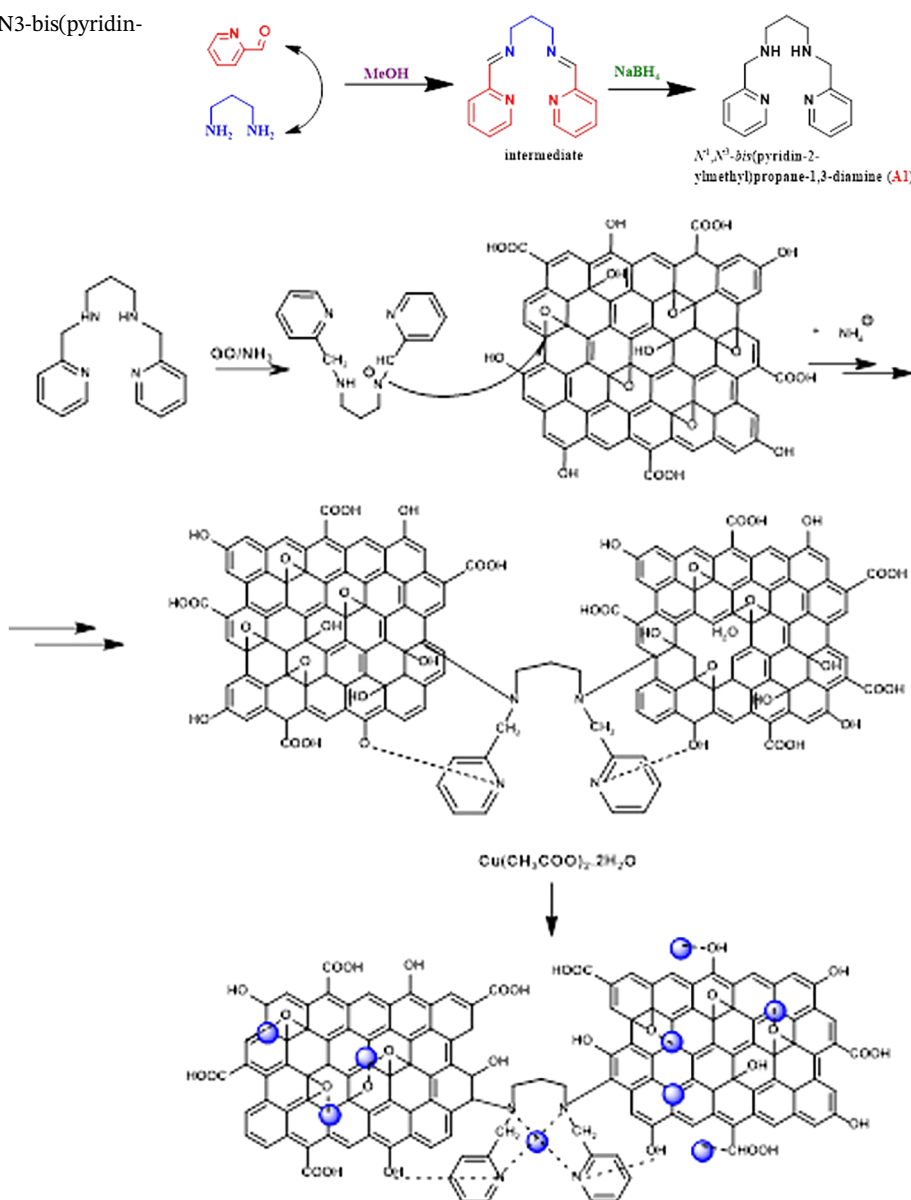


SCHM E 1 General synthesis of ethyl-5,7-diamino-6-cyano-2-methyl-4-(3-nitrophenyl)-4H-pyranopyridine-3-carboxylate

2.3 | Preparation of N-ligand (A1)

For the preparation of **A1**, 5 mmol (0/37 g) propylenediamine was added to a solution of 10 mmol (1.07 g) pyridine-2-carbaldehyde in a dry methanol solution and the solution was refluxed for 12 hr. As a result, it opened up the Schiff as an intermediate product. In the next step, 40 mmol (1.51 g) of sodium borohydride was added to the above solution for 2 hr and sprayed into the ice bath for 48 hr. After completion of the reaction time, **A1** was separated from water and chloroform (Scheme 3).

SCHEME 3 Schematic structure of N1,N3-bis(pyridin-2-ylmethyl)propane-1,3-diamine (N-Ligand)



SCHEME 4 Schematic structure of GO/N-Ligand-Cu

2.4 | Preparation of GO/N-ligand-cu nanocomposite

GO (1 g) was spread in 250 ml distilled water through stirring by using bath ultrasonication for 30 min. The GO spreading was done to a 250 ml three-necked and round end flask with a magnetic stirrer, and a reflux condenser, then 4 g (15.6 mmol) *N*-Ligand and 6 ml ammonia were added to the flask and the mixture was stirred for 24 hr under reflux condition. Afterwards, the resulted (GO/*N*-Ligand) was filtrated and cleaned by hot water and ethanol to get rid of unreacted elements. Then, this mixture was sealed by filtration and dried in an oven at 100 °C for 24 hr. Dispersing 2 g GO/*N*-Ligand in 100 ml ethanol

was attained through ultrasonication for 15 min. Successively, 1 g cupric acetate was added to the mixture, then stirred at reflux for 24 hr. The product was completely washed with hot ethanol for many times. The obtained GO/N-Ligand-Cu was dried at 80 °C for 24 hr. The synthetic way is shown in Scheme 4.^[3,23]

2.5 | Preparation of chromeno[2,3-*b*]pyridine: General procedure

A blend of the aldehyde (1 mmol), malononitrile (2 mmol), ethyl acetoacetate (1 mmol) and GO/N-Ligand-Cu nanocomposites catalyst (0.05 g), in water (3 ml) was refluxed for. The development of the reaction was followed by TLC (*n*-hexane/acetone, 7:3). After the completion of the reaction, the resulting precipitate was filtered to eliminate the catalyst and the crude product was recrystallized from ethanol to get the pure compound. The products were characterized using physical and spectroscopic (NMR, Ms) data (Supporting Information Data S1–S2).

2.6 | Evaluation of copper removal from GO/N-ligand-cu catalyst surface in chromeno[2,3-*b*]pyridine synthesis

Methyl 5,7-diamino-6-cyano-2-methyl-4-(4-nitrophenyl)-4*H*-pyrano[2,3-*b*]pyridine-3-carboxylate derivative was selected as the sample for this test. After 50 percent reaction progress (15 min), the reaction was stopped, the reaction was stopped and the catalyst was separated from the reaction mixture by centrifugation. The reaction mixture was placed under the same conditions for 15 min after separation of the catalyst and no significant progress was observed in the reaction process. The results of this test showed that copper nanocomposites were not released in the reaction medium and remained on the surface of the catalyst and as well as the catalyst was very stable in contrast to moisture, air and reaction conditions.

2.7 | Analytical data of the selected products

2.7.1 | Methyl 5,7-diamino-6-cyano-2-methyl-4-(4-nitrophenyl)-4*H*-pyrano[2,3-*b*]pyridine-3-carboxylate (4a)

Light yellow solid; Yield: 94% (940 mmol); M.p: 220–223 °C. ¹H NMR (400 MHz, DMSO-*d*₆): δ 1.20–2.53 (t, 3H, CH₃), 4.19 (q, 2H, CH₂), 4.65 (s, 1H, CH), 7.38–7.40 (d, *J* = 8 Hz, 2H, ArH), 7.83 (s, 2H,

NH₂), 8.06–8.08 (d, *J* = 8 Hz, 2H, ArH), 8.79 (s, 2H, NH₂); ¹³C NMR (100 MHz, DMSO-*d*₆): δ 14.9, 17.3, 36.3, 62.8, 69.3, 104.1, 106.7, 112.2, 116.7, 119.2, 129.3, 137.2, 154.8, 159.3, 164.5, 167.7, 170.0; MS (m/z): 380.25 (M⁺, 100%), 367.35, 350.2, 340.7, 335.15, 295.9, 281.05, 225.

2.7.2 | Methyl 5,7-diamino-6-cyano-4-(2-hydroxyphenyl)-2-methyl-4*H*-pyrano[2,3-*b*]pyridine-3-carboxylate (4b)

Light yellow solid; Yield: 93% (930 mmol); M.p: 196–200 °C. ¹H NMR (250 MHz, DMSO-*d*₆): δ 1.14 (t, 3H, CH₃), 2.28 (s, 3H, CH₃), 3.97 (q, 2H, CH₂), 5.34 (s, 1H, CH), 6.56 (s, 2H, NH₂), 6.65–6.69 (d, *J* = 10, 1H, ArH), 7.02–7.12 (m, 2H, ArH), 7.23–7.27 (d, *J* = 10, 1H, ArH), 7.66 (s, 2H, NH₂), 9.44 (s, 1H, OH); ¹³C NMR (62.5 MHz, DMSO-*d*₆): δ 14.9, 17.3, 36.3, 62.8, 64.9, 104.1, 106.8, 109.5, 112.5, 116.7, 119.2, 128.6, 137.2, 153.4, 154.8, 159.3, 164.5, 167.7, 170.0; MS (m/z): 366.3 (M⁺, 100%), 360.3, 350.1, 338.2, 320/2, 295.2, 225.3, 106.1.

2.7.3 | Methyl 5,7-diamino-6-cyano-4-(2-methoxyphenyl)-2-methyl-4*H*-pyrano[2,3-*b*]pyridine-3-carboxylate (4c)

Light yellow solid; Yield: 90% (900 mmol); M.p: 216–218 °C. ¹H NMR (250 MHz, DMSO-*d*₆): δ 1.15–1.20 (t, 3H, CH₃), 2.28 (s, 3H, CH₃), 3.81 (s, 3H, OCH₃), 3.97 (q, 2H, CH₂), 4.98 (s, 1H, CH), 6.12 (s, 2H, NH₂), 7.00–7.07 (m, 3H, ArH), 7.30–7.34 (d, *J* = 10, 2H, ArH), 8.29 (s, 2H, NH₂); ¹³C NMR (62.5 MHz, DMSO-*d*₆): δ 14.3, 19.1, 21.5, 56.0, 60.1, 61.3, 79.5, 112.1, 113.8, 115.6, 121.3, 126.3, 129.1, 130.1, 138.5, 148.1, 151.6, 157.6, 164.5, 166.2; MS (m/z): 380.7 (M⁺, 100%), 352.8, 350.6, 301.7, 222, 184.05, 151.0.

2.7.4 | Methyl 5,7-diamino-6-cyano-2-methyl-4-(*m*-tolyl)-4*H*-pyrano[2,3-*b*]pyridine-3-carboxylate (4d)

Light yellow solid; Yield: 91% (910 mmol); M.p: 220–224 °C. ¹H NMR (250 MHz, DMSO-*d*₆): δ 1.23 (t, 3H, CH₃), 1.93 (s, 3H, CH₃), 2.47 (s, 3H, CH₃), 4.23 (q, 2H, CH₂), 4.93 (s, 1H, CH), 6.11 (s, 2H, NH₂), 7.20–7.27 (m, 1H, ArH), 7.30 (s, 1H, ArH), 7.42–7.44 (m, 2H, ArH), 9.21 (s, 2H, NH₂); ¹³C NMR (62.5 MHz, DMSO-*d*₆): δ 14.2, 20.7, 21.5, 48.2, 63.1, 64.2, 102.9, 113.4, 116.6, 125.7, 129.1, 130.2, 131.7, 136.9, 138.3, 158.9, 162.9, 163.9, 164.6, 164.9; MS (m/z): 364.4 (M⁺, 100%), 350, 320.15, 233.95, 231.95, 172.1, 153.1.

2.7.5 | Methyl 5,7-diamino-6-cyano-4-(4-fluorophenyl)-2-methyl-4*H*-pyrano[2,3-*b*]pyridine-3-carboxylate (4e)

Light yellow solid; Yield: 91% (910 mmol); M.p: 210–212 °C. ¹H NMR (250 MHz, DMSO-*d*₆): δ 1.33 (t, 3H, CH₃), 3.08 (s, 3H, CH₃), 4.12 (q, 2H, CH₂), 4.99 (s, 1H, CH), 6.18 (s, 2H, NH₂), 6.82–6.86 (d, *J* = 10 Hz, 2H, ArH), 7.80–7.84 (d, *J* = 10 Hz, 2H, ArH), 8.03 (s, 2H, NH₂); ¹³C NMR (62.5 MHz, DMSO-*d*₆): δ 14.9, 17.3, 36.3, 62.8, 69.3, 104.1, 106.7, 112.2, 116.7, 119.2, 137.2, 154.8, 159.3, 164.5, 167.7, 170.0; MS (m/z): 370.9 (M⁺, 100%), 369.55, 350.1, 294.3, 280.2.

2.7.6 | Methyl 5,7-diamino-6-cyano-4-(2,4-dichlorophenyl)-2-methyl-4*H*-pyrano[2,3-*b*]pyridine-3-carboxylate (4f)

Light yellow solid; Yield: 89% (890 mmol); M.p: 218–220 °C. ¹H NMR (250 MHz, DMSO-*d*₆): δ 1.13 (t, 3H, CH₃), 2.61 (s, 3H, CH₃), 3.99 (q, 2H, CH₂), 5.38 (s, 1H, CH), 6.14 (s, 2H, NH₂), 7.00 (s, 2H, NH₂), 7.02 (s, 1H, ArH), 7.17 (1H, ArH), 7.40 (1H, ArH); ¹³C NMR (62.5 MHz, DMSO-*d*₆): δ 14.9, 17.3, 36.3, 61.3, 62.8, 104.1, 106.7, 112.2, 124.9, 130.4, 132.0, 137.2, 140.4, 142.6, 154.8, 159.3, 164.5, 167.7, 170.0; MS (m/z): 420.95 (M⁺, 100%), 419.45, 418, 398, 378.8, 350.2, 155.1.

2.7.7 | Ethyl 5,7-diamino-4-(4-chlorophenyl)-6-cyano-2-methyl-4*H*-pyrano[2,3-*b*]pyridine-3-carboxylate (4 g)

Light yellow solid; Yield: 91% (910 mmol); M.p: 225–229 °C. ¹H NMR (400 MHz, DMSO-*d*₆): δ 1.21 (t, 3H, CH₃), 2.18 (s, 3H, CH₃), 4.22 (q, 2H, CH₂), 4.97 (s, 1H, CH), 7.12 (s, 2H, NH₂), 7.49–7.51 (d, *J* = 8 Hz, 2H, ArH), 7.75 (s, 2H, NH₂), 7.89–7.91 (d, *J* = 8 Hz, 2H, ArH); ¹³C NMR (62.5 MHz, DMSO-*d*₆): δ 8.7, 13.82, 14.1, 56.9, 61.5, 61.7, 111.2, 113.9, 128.1, 129.2, 129.5, 129.9, 131.0, 131.1, 132.3, 140.3, 159.9, 191.2; MS (m/z): 386.35 (M⁺, 100%), 384, 369.9, 350.7, 329.4, 322.5, 295.2, 229.2, 191.1, 159.1, 153.05.

2.7.8 | Ethyl 5,7-diamino-4-(4-bromophenyl)-6-cyano-2-methyl-4*H*-pyrano[2,3-*b*]pyridine-3-carboxylate (4 h)

Light yellow solid; Yield: 90% (900 mmol); M.p: 225–228 °C. ¹H NMR (400 MHz, DMSO-*d*₆): δ 1.10 (t, 3H, CH₃), 2.19 (s, 3H, CH₃), 4.13 (q, 2H, CH₂), 5.00 (s, 1H,

CH), 7.31 (s, 2H, NH₂), 7.49 (s, 2H, NH₂), 7.65–7.67 (d, *J* = 8 Hz, 2H, ArH), 8.12–8.14 (d, *J* = 8 Hz, 2H, ArH); ¹³C NMR (100 MHz, DMSO-*d*₆): δ 18.6, 19.2, 31.7, 57.1, 61.1, 82.7, 110.9, 112.7, 113.8, 129.4, 130.2, 131.06, 131.1, 132.2, 132.4, 132.9, 159, 160; MS (m/z): 430.2(M⁺, 100%), 431.8, 428.3, 399.25, 350.2, 322.4, 233, 232, 159.1.

2.7.9 | Ethyl 5,7-diamino-6-cyano-4-(4-methoxyphenyl)-2-methyl-4*H*-pyrano[2,3-*b*]pyridine-3-carboxylate (4i)

Light yellow solid; Yield: 91% (910 mmol); M.p: 230–233 °C. ¹H NMR (400 MHz, DMSO-*d*₆): δ 1.21 (t, 3H, CH₃), 2.53 (s, 3H, CH₃), 3.86 (s, 3H, OCH₃), 4.17(q, 2H, CH₂), 5.00 (s, 1H, CH), 7.77–7.79 (d, *J* = 8 Hz, 2H, ArH), 7.90–7.92 (d, *J* = 8 Hz, 2H, ArH), 7.98 (s, 2H, NH₂), 9.31 (s, 2H, NH₂); ¹³C NMR (100 MHz, DMSO-*d*₆): δ 14.2, 25.7, 29.6, 55.3, 55.8, 55.9, 113.8, 114.2, 114.5, 114.7, 115.2, 124.3, 130, 132, 133.7, 160.02, 164.6, 164.8, 190.8; MS (m/z): 380.15(M⁺, 100%), 350.1, 320.8, 286.12, 221.25, 184.

2.7.10 | Ethyl 5,7-diamino-6-cyano-2-methyl-4-(*p*-tolyl)-4*H*-pyrano[2,3-*b*]pyridine-3-carboxylate (4j)

Light yellow solid; Yield: 89% (890 mmol); M.p: 220–223 °C. ¹H NMR (400 MHz, DMSO-*d*₆): δ 1.20 (t, 3H, CH₃), 2.43 (s, 6H, CH₃), 4.10 (q, 2H, CH₂), 4.46 (s, 1H, CH), 7.03 (s, 2H, NH₂), 7.45–7.47 (d, *J* = 8 Hz, 2H, ArH), 7.88–7.90 (d, *J* = 8 Hz, 2H, ArH), 8.49 (s, 2H, NH₂); ¹³C NMR (100 MHz, DMSO-*d*₆): δ 8.9, 14.5, 21.9, 57.1, 61.1, 80.42, 114, 114.9, 129.2, 129.6, 129.8, 130.1, 130.6, 131.2, 134.6, 148.2, 161.8; MS (m/z): 364.4(M⁺, 100%), 350, 320.15, 233.95, 231.95, 172.1.

3 | RESULT AND DISCUSSION

The initial stage for the chromeno[2,3-*b*]pyridine synthetic approach is related to the development of the reaction conditions and examination of the catalytic activity of GO/N-Ligand-Cu nanocomposites. So that outline the optimization conditions of the reaction, the catalytic activity of several catalysts was studied in the exemplary reaction.

The selection of catalyst has a high significance for the reproduction of chromeno[2,3-*b*] pyridine, consequently, the effect of several solvents, as well as of various reaction temperature on the reaction of aldehydes **1**, 1,3-diketone **2** and malononitrile **3** has been investigated.

TABLE 1 Catalytic activity of different catalysts on the synthesis of chromeno[2,3-*b*]pyridine^a

Entry	Catalyst	Solvent	Time (min)	T (°C)	Yield ^b (%)
1	No catalyst	H ₂ O	1440	100	-
2	Chitosan@citric acid	CH ₃ CH ₂ OH	-	reflux	94
3	DMAP	H ₂ O	-	reflux	90
4	Fe ₃ O ₄ @SiO ₂ -NH ₂	H ₂ O/EtOH	-	reflux	97
5	Et ₃ N	PrOH	-	98	98
6	GO/N-Ligand-Cu	H ₂ O	30	reflux	94
7	GO/N-Ligand-Cu	Solvent-free	260	100	78
8	GO/N-Ligand-Cu	CH ₃ CH ₂ OH	160	80	85
9	GO/N-Ligand-Cu	CHCl ₃	210	65	88
10	GO/N-Ligand-Cu	H ₂ O	1440	r.t	20
11	GO/N-Ligand-Cu	H ₂ O	1440	50	35
12	GO/N-Ligand-Cu	H ₂ O	1440	75	53
13	GO	H ₂ O	720	reflux	20
14	GO/Cu	H ₂ O	720	reflux	25
15	<i>N</i> -Ligand-Cu	H ₂ O	720	reflux	34

^aReaction conditions: 4-nitro benzaldehyde (1 mmol), malononitrile (2 mmol), ethyl acetoacetate (1 mmol), solvent (5 mL), GO/N-Ligand-Cu (0.05 g).

^bIsolated yield.

The catalytic results of various catalysts are displayed in Table 1. It was verified by the outcomes once the reaction is done without catalyst (Table 1, entry 1). Regardless of the protracted reaction time, no product is obtained, therefore it is highlighting the specific role of catalyst. To investigate the effect of temperature on the reaction, we performed the model reaction at r.t, 50 °C, 75 °C, and reflux conditions (Table 1, entries 6 and 10–12). The examination of the temperature showed that reflux conditions proved to be the best. Thus, we determined our best circumstances as shown in entry 6.

In the presence of catalysts such as Chitosan@citric acid,^[24] DMAP,^[25] Fe₃O₄@SiO₂-NH₂^[26] and Et₃N,^[18] application of high hazardous, odorous and expensive materials such as thiols and alkyl phosphite ester is a disadvantage of previous methods (Table 1, entries 2–5).

These observations resulted in finding measures and means to decrease the time and cost of consumption. Thus, it looks practical to think that we could use a

dissimilar catalyst such as GO/N-Ligand-Cu, and also water would be a good option as a green solvent.

To further compare this method, we also performed the model reaction in the presence of different catalysts. After the reaction, it was found that the catalyst used in this report performed better than other catalysts (Table 2, entries 1–4).^[21,27,28]

Combining many compounds of 4-nitro benzaldehyde **1**, ethyl acetoacetate **2** and malononitrile **3**, chromeno[2,3-*b*]pyridines **4(a-j)** was synthesized. We realized that the reaction in the existence of GO/N-Ligand-Cu increased the wanted product (96%) in less reaction time (00:30 min) (Table 1, entries 6). The solvent has a noticeable effect on the production and reaction time (Table 1, entries 9–12) and the finest outcome was attained in water solvent conditions. Additionally, we also studied the influence of temperature (Table 1, entries 6–9). To investigate the effect of the catalyst on the reaction, we designed a reaction in which the effects of GO, GO/Cu^[29] and *N*-ligand-Cu were studied separately.

TABLE 2 Effect of various catalysts on yield of chromeno[2,3-*b*]pyridine

Entry	Catalyst (g)	T (°C)	Time (min)	Yield (%)	Ref.
1	LDHs@Propyl-ANDSA (0.05)	Reflux	50	68	1
2	LDH/Tris/Pd. (0.05)	Reflux	45	82	2
3	Fe ₃ O ₄ @SiO ₂ @Propyl-ANDSA (0.05)	Reflux	65	70	3
4	GO/N-Ligand-Cu (0.05)	Reflux	30	94	In work

According to the results (Table 1, entries 13–15), it did not have much effect on the reaction progress, confirming that the GO/N-Ligand-Cu catalyst worked well and increased the efficiency and reduced reaction time without side products. The oxidation state of Cu in GO/N-ligand-Cu and cupric acetate on graphene oxide nanoparticles is Cu (II), But once copper was deposited

on the GO/N-Ligand, in fact, greater amounts of copper were placed on the surface of the catalyst.

As a result, the reaction rate is increased compared to when we used N¹,N³-bis (pyridin-2-ylmethyl) propane-1,3-diamine and cupric acetate on graphene oxide nanoparticles composite.

Also, amount of catalyst (Table 3) in water solvent situations. There was considerable growth in the production by a rise in the reaction temperature.

As a result, a reflux for 00:30 min in water solvent condition in the presence of 0.05 g catalyst is identified as the ideal reaction condition. It is thought that a nano-structure can be a good troth as a catalyst because of their surface area developments strictly.

The catalyst activity of GO/N-Ligand-Cu apparently is associated to: (1) nanostructured nature of the catalyst and (2) catalytic activity of copper metal for triggering the starting materials. The ideal amount of nano-catalyst loading in this reaction, was measured to be 0.05 g (Table 3, entry 3). By decreasing the catalyst loading to 0.025 g, the preferred product was acquired in low yield (Table 2, entries 1) while with increasing of the catalyst

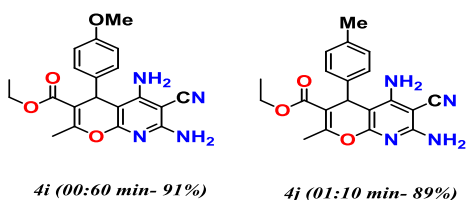
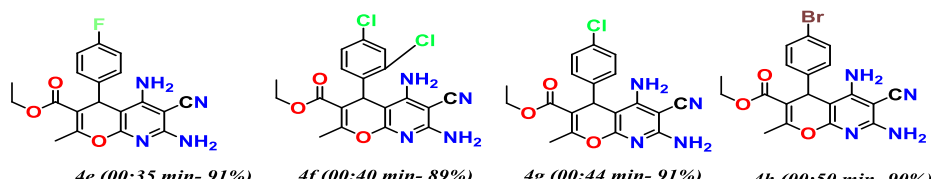
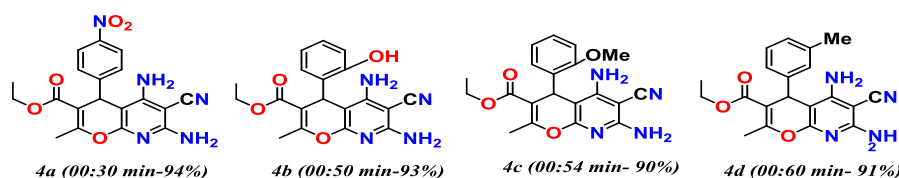
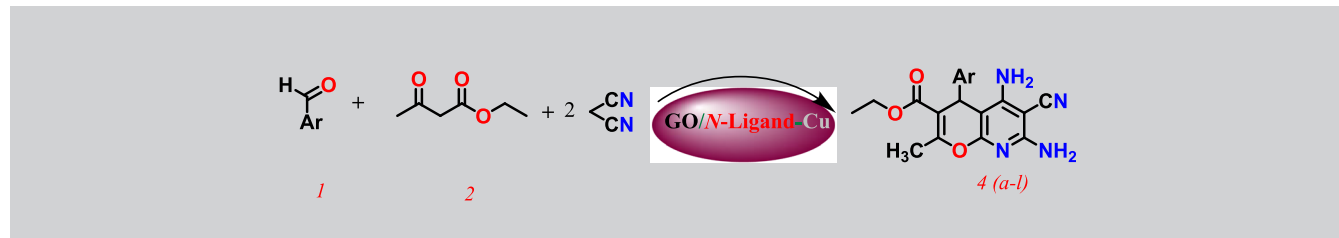
TABLE 3 Effect of catalyst amount on the reaction between 4-nitro benzaldehyde (1 mmol), malononitrile (2 mmol), ethyl acetoacetate (1 mmol)^a

Entry	Amount of cat. (g)	Yield ^b (%)
1	0.025	35
2	0.03	84
3	0.05	94
4	0.1	96

^aReaction conditions: 4-nitro benzaldehyde (1 mmol), malononitrile (2 mmol), ethyl acetoacetate (1 mmol), H₂O (5 mL), GO/N-Ligand-Cu (0.05 g).

^bIsolated yield.

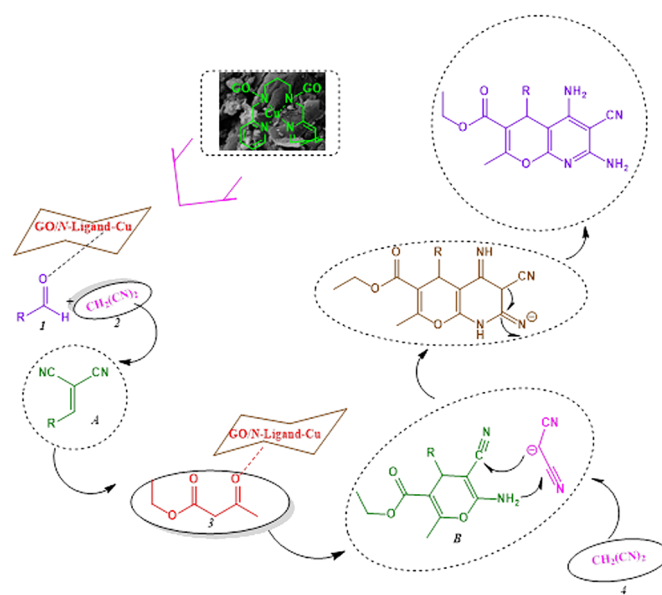
TABLE 4 Synthesis of chromeno[2,3-*b*]pyridine derivatives using GO/N-Ligand-Cu as a catalyst^a



^aReaction conditions aldehyde (1 mmol), malononitrile (2 mmol), ethyl acetoacetate (1 mmol), H₂O (5 mL), GO/N-ligand-Cu (0.05 g).

loading to 0.1 g has no significant effect on reaction rate and isolated yield of product (Table 3, entry 4).

Many methods directed towards the synthesis of methyl-5,7-diamino-6-cyano-2-methyl-4-(3-nitrophenyl)-4*H*-pyrano[2,3-*b*]pyridine-3-carboxylate have therefore been developed; this method has attracted much interest concerning the available methods catalyzed by different



SCHEME 5 Suggested mechanism for the synthesis of chromeno[2,3-*b*]pyridine catalyzed by GO/N-Ligand-Cu

catalysts; because this method was undertaken at 100 °C, with high yields in short reaction time.

It can be seen that 89–94% yield of products is obtained at 100 °C in the presence of 0.05 g GO/N-Ligand-Cu after 00:35 to 1:40 min (Table 4).

As an attempt to expand the range of our method, afterward, we used several aldehydes as the substrates for this reaction. The items in Table 4 reveal that the catalysis progressed well for a wider variety of aryl aldehydes, given that the corresponding chromeno[2,3-*b*]pyridine to be in high yields. The results indicated that an electron-donating group or an electron-withdrawing group on aryl aldehydes does not have a distinguished outcome and

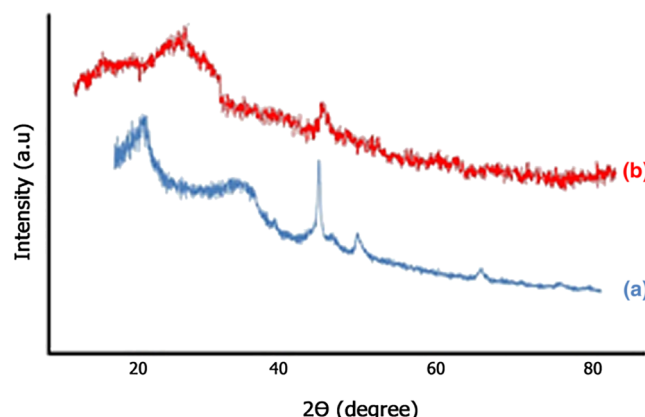


FIGURE 2 XRD patterns: a) GO, b) GO/N-Ligand-Cu

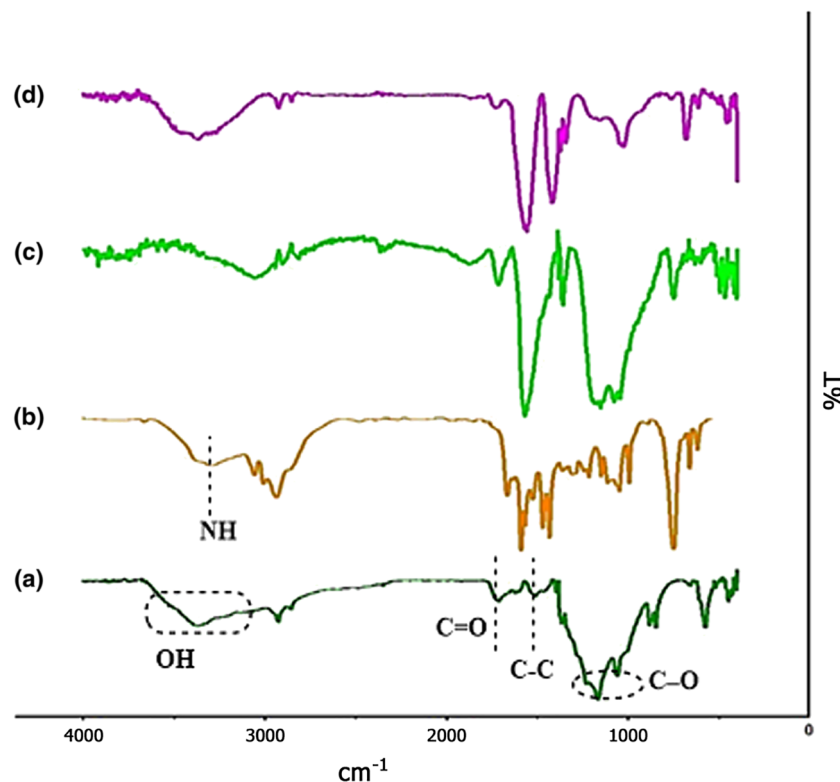


FIGURE 1 FT-IR spectra: a) GO, b) N-Ligand, c) GO/N-Ligand, d) GO/N-Ligand-Cu

gives proper yields. Thus, the best acting catalyst to reach methyl-5,7-diamino-6-cyano-2-methyl-4-(4-nitrophenyl)-4*H*-pyrano[2,3-*b*]pyridine-3-carboxylate is the nano GO/*N*-Ligand-Cu catalyst, causes great yields of up to 94%. The recognized compounds were described by their physical and spectral data in comparison with the reports in the literature.

Considering the achieved data and our current results on the multicomponent synthesis of chromeno[2,3-*b*]pyridine from aldehydes, malononitrile and ethyl acetoacetate the succeeding scheme for the synthesis of chromeno[2,3-*b*]pyridine is proposed (Scheme 5). Knoevenagel condensation of aldehyde **1** and malononitrile **2** is the first step of the domino process. Subsequently, the Michael addition of ethyl acetoacetate **3** to intermediate **A** provides the intermediate **B** which then undergoes tautomerization and later intramolecular cyclization twice, lastly, the addition of another correspondent of malononitrile **4** leads into chromeno[2,3-*b*]pyridine.

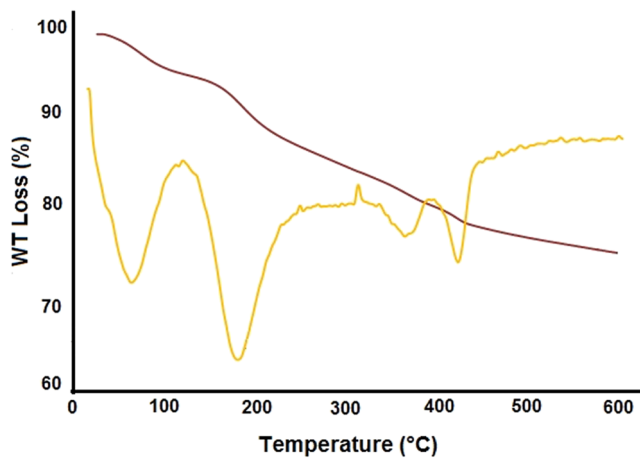


FIGURE 3 TGA curve of GO/N-Ligand-Cu

GO/*N*-Ligand-Cu nanocomposites as a novel catalyst was prepared based on the subsequent procedure (Scheme 1) (see the experimental section).

The properties of GO/*N*-Ligand-Cu catalyst were approved several microscopic and spectroscopic methods like transmission electron microscopy (TEM), scanning electron microscopy (SEM), thermal gravimetric analysis (TGA), X-ray diffraction (XRD) and FT-IR spectroscopies. Inductively coupled plasma optical emission spectroscopy (ICP/OES) analysis of the catalyst found that the weight percentage of Cu to be 25.8 wt% Cu in the catalyst.

Firstly, we utilized the FT-IR spectrum to describe the functionalized GO/N-Ligand-Cu. The FT-IR spectrum of graphene oxide, *N*-Ligand and functionalized GO/N-Ligand-Cu are presented in Figure 1. The results reveal that the characteristic bands of badge GO are detected at 1725 cm⁻¹ (C=O stretching in carboxylic acid), 1622 cm⁻¹ (C-C stretching in the aromatic ring), 1230 cm⁻¹ (C-O stretching in epoxy), and 1060 cm⁻¹ (C-O stretching in alkoxy). Two absorption bands about 3290 cm⁻¹ and 1354 cm⁻¹ were related to the NH stretching vibrations and the bending vibration absorption peak of N-H. On the other hand, after functionalization, the bending vibration absorption peak of N-H at about 3290 cm⁻¹ vanished or shifted, which was shown as the copper coordination of the ligand.

The X-ray diffraction pattern of graphene oxide nanosheets and after GO/N-Ligand-Cu is shown in Figure 2.

As can be seen in spectrum a, the peak values of $2\theta = 25^\circ$ and 45° , correspond to the standard XRD spectrum of graphene oxide nanosheets and in Figure b, the indicator peak with values of 25° , 35° , 43° , 55° and 72° confirms the presence of Cu on graphene oxide nanoparticles (35° , 55° , 72° peaks of copper metal).

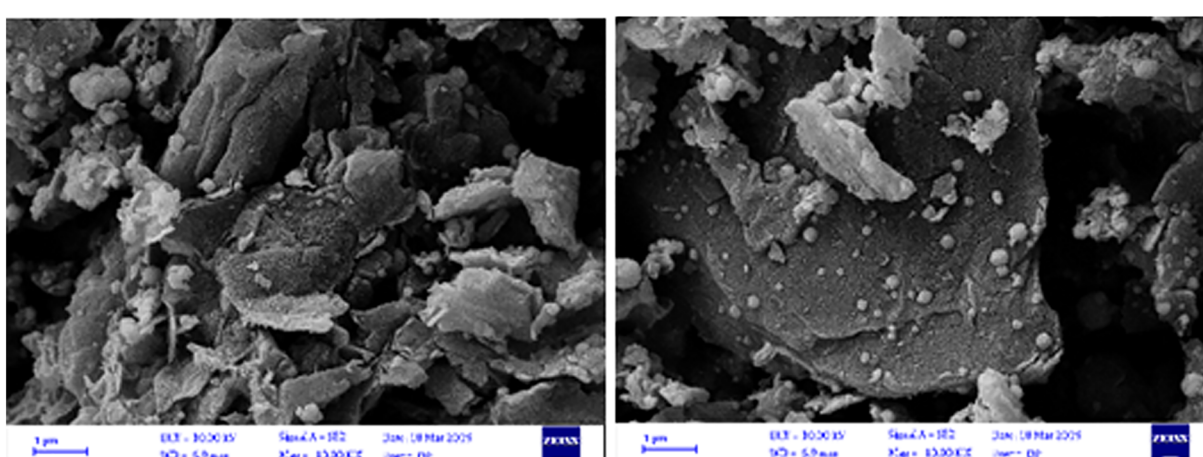


FIGURE 4 SEM of GO/N-Ligand-Cu

The thermal decomposition of GO, GO/N-Ligand-Cu was investigated by using thermogravimetric methods. The thermogram was documented in the temperature ranges of 25–600 °C with a heating rate of 10 degrees per minute. The data from the thermogravimetric analysis

obviously shows that the degradation of the catalyst continues in three stages and the parallel spectrum is presented in Figure 3.

In the TGA and DTG thermogram, the first weight loss is about 25–50 as a result of the loss of water mole-

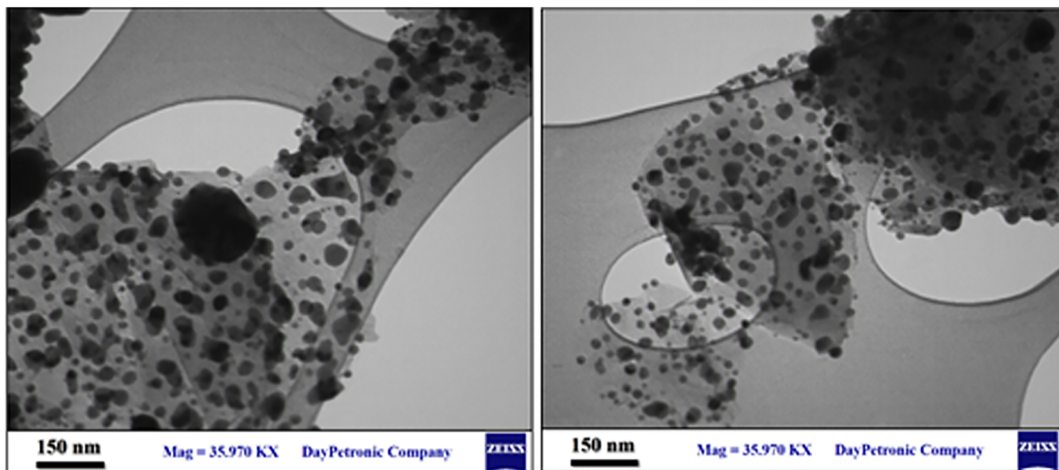


FIGURE 5 TEM of GO/N-Ligand-Cu

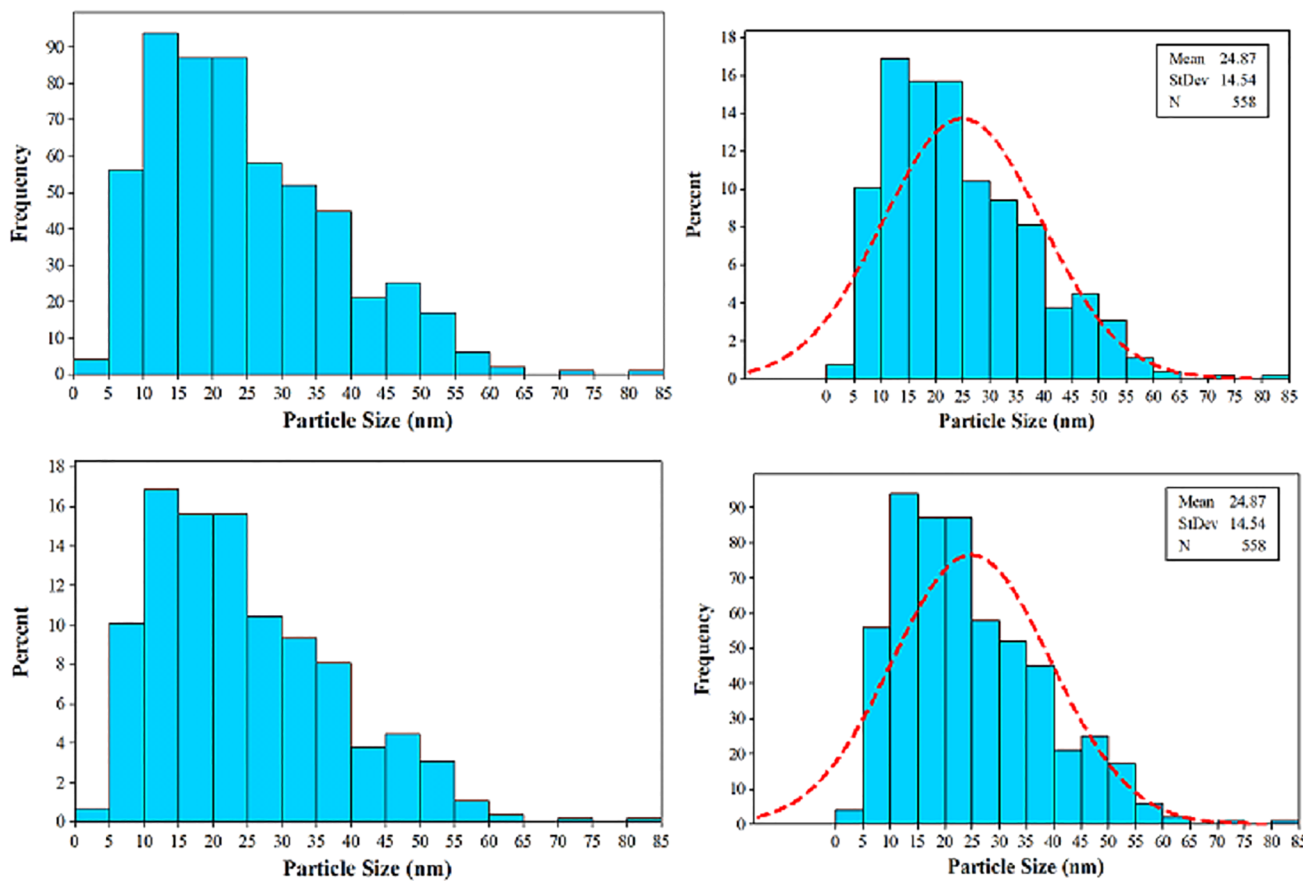


FIGURE 6 The particle size distribution histograms of the GO/N-Ligand-Cu

cules and dopant, the second decomposition in the temperature range 50–130 is because of the loss of copper metal and the third weight loss occurred from 130–250 is because of the degradation of *N*-Ligand and the final weight loss related to GO.

By using SEM and TEM the morphology of the GO/*N*-Ligand-Cu is investigated, they are shown in Figures 3 and 4. The morphology and structure (SEM) of the GO/*N*-Ligand-Cu nanosheets are illustrated in Figure 4. The image of the GO formed showed thin and wrinkle nanosheets. Moreover, the SEM images of GO/*N*-Ligand-Cu was verified that the catalyst was composed of uniform nanometer-sized particles.^[30]

It is observable that GO/*N*-Ligand-Cu wrinkles and can be recognized to the folding of the sheets as shown in the TEM image. You may describe this by the thermodynamic instability of exfoliated 2-D structure of GO sheets along with the van der Waals attractions between the graphene oxide layers (Figure 5).

The exfoliated GO sheets are joined to each other to make thick layers become steady because of the thermodynamic instability. Furthermore, the incidence of

oxygen functional group in the GO layers also play part in its thermal variability at high temperature. Additionally, TEM pictures show that Cu nanoparticles were distributed consistently on the graphene plane.^[31]

At a closer look, as shown in the particle size distribution histograms (Figure 6), the sizes of the nanoparticles are between 5–40 nm and the average particle size is estimated at about 24.87 nm, while more than 70% of the catalyst particles have an average size of about 5–55 nm.

The EDX data for the GO/*N*-Ligand-Cu (Figure 7) verified the existence of the anticipated elements carbon, oxygen, nitrogen, and especially copper in the catalyst.

The scheme and mixture of recoverable catalysts is a really difficult interdisciplinary field of study, it needs incorporating chemistry, the science of materials engineering, economics and environmental purposes. Considering the proper outcomes achieved from the catalyst activity throughout the reaction, we made a decision to examine the catalyst constancy by examining their recyclability and activity in the experiment. By using

FIGURE 7 EDX of GO/*N*-Ligand-Cu

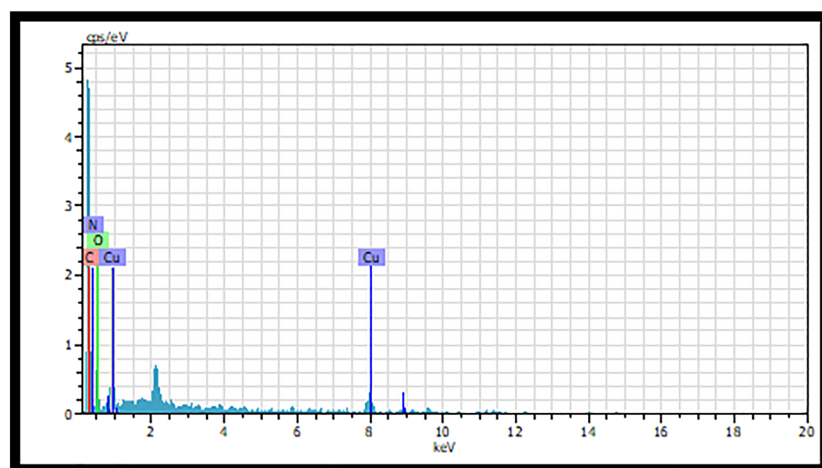
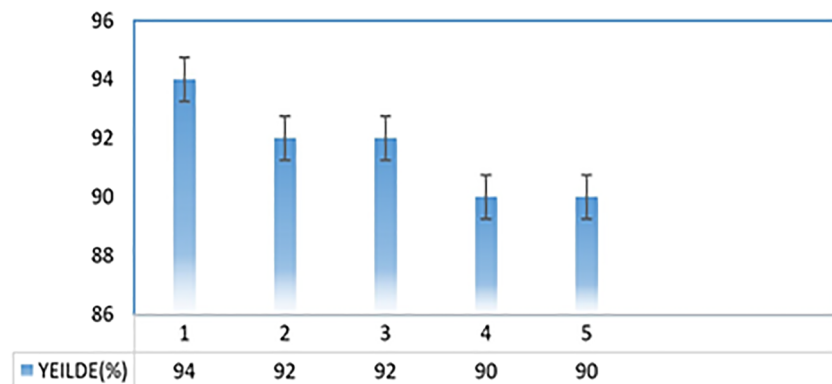


FIGURE 8 Recyclability test of GO/*N*-Ligand-Cu



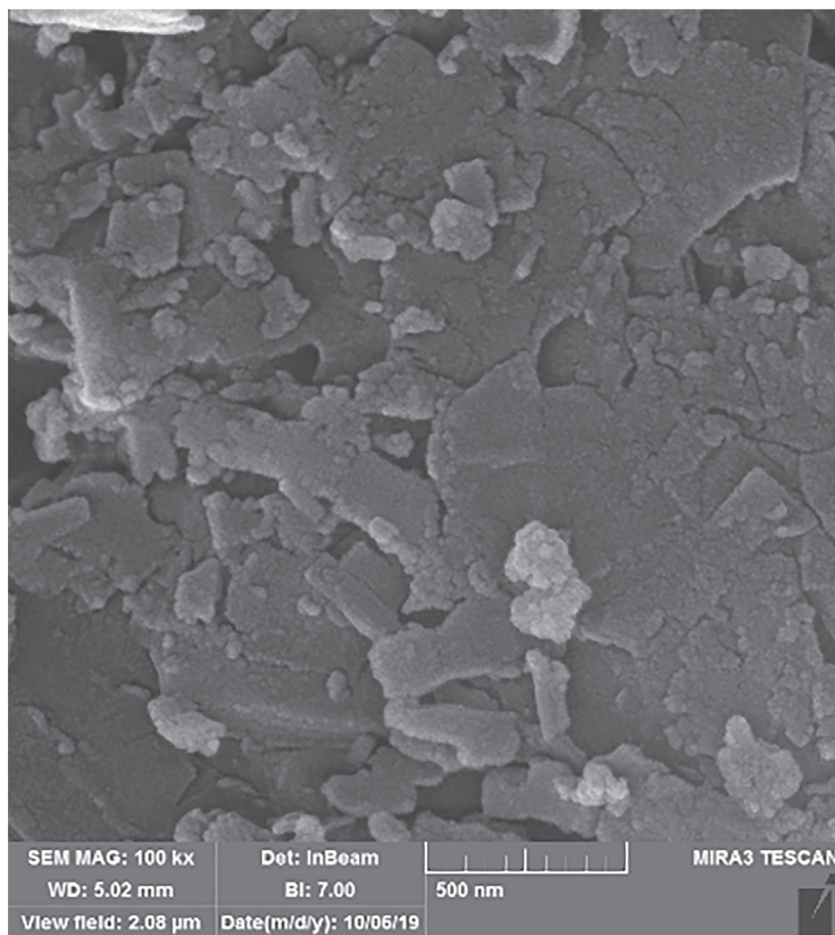


FIGURE 9 SEM Spectrum of catalyst after use GO/N-Ligand-Cu

4-nitrobenzaldehyde as the model substrate, recycling research was executed. The reaction situations utilized in these experiments were equal to the described experiments; besides the reaction development was examined by TLC. Following completing each course (45 min), the reaction combination was permitted to get room temperature, and the solid catalyst was divided by centrifugation, washed with acetone, dried, and used again in the later run. This practice might be conducted 5 times with no noticeable variation in the product. It shows similar action in each run without any remarkable loss of its catalytic activity (Figure 8).

In the first run, 94% GO/N-Ligand-Cu was recycled, and the pureness and structure of recovered GO/N-Ligand-Cu remain unchanged on the basis of the SEM result (Figure 9).

CONCLUSIONS

Multicomponent procedures show important superiorities over old step by step methods, for instance, easier synthetic processes, lower costs, environmentally friendly, effectiveness, and great bond-forming effectiveness. By the way, the impression of heterocycles on

MCRs has been newly investigated and establishes an active study area. Moreover, in this paper, a new catalyst synthesized by *N^{1,N³}*-bis (pyridin-2-ylmethyl)propane-1,3-diamine and cupric acetate on graphene oxide nanoparticles composite were used for chromeno[2,3-*b*]pyridines.

This nanocomposite profits from favorable extraction qualities of graphene oxide (high surface field and worthy extraction ability) and time-saving. Ultimately, this process was utilized for the synthesis of chromeno[2,3-*b*]pyridines and satisfactory outcomes were acquired.

ACKNOWLEDGEMENT

The authors wish to thank Bu-Ali Sina University, Center of Excellence Developmental of Environmentally Friendly Methods for Chemical Synthesis (CEDEFMCS).

ORCID

Zahra Karamshahi <https://orcid.org/0000-0003-2777-6629>
 Ramin Ghorbani-Vaghei <https://orcid.org/0000-0001-8322-6299>

Hassan Keypour  <https://orcid.org/0000-0001-9973-241X>
 Mohammad Taher Rezaei  <https://orcid.org/0000-0001-9386-6126>

REFERENCES

- [1] M. Baghayeri, H. Alinezhad, M. Fayazi, M. Tarahomi, R. Ghanei-Motlagh, B. Maleki, *Electrochim. Acta* **2019**, 312, 80.
- [2] H. Alinezhad, M. Tarahomi, B. Maleki, A. Amiri, *Appl. Organomet. Chem.* **2019**, 33, 4661.
- [3] B. Yuan, C. Bao, L. Song, N. Hong, K. M. Liew, Y. Hu, *Chem. Eng. J.* **2014**, 237, 411.
- [4] K. S. Novoselov, A. K. Geim, S. Morozov, D. Jiang, M. Katsnelson, I. Grigorieva, S. Dubonos, A. A. Firsov, *Nature* **2005**, 438, 197.
- [5] H. Yu, B. Zhang, C. Bulin, R. Li, R. Xing, *Sci. Rep.* **2016**, 6, 36143.
- [6] M. Tarahomi, H. Alinezhad, B. Maleki, *Appl. Organomet. Chem.* **2019**, 33, 5203.
- [7] Y. Xu, Z. Liu, X. Zhang, Y. Wang, J. Tian, Y. Huang, Y. Ma, X. Zhang, Y. Chen, *Adv. Mater.* **2009**, 21, 1275.
- [8] H. K. F. Cheng, N. G. Sahoo, Y. P. Tan, Y. Pan, H. Bao, L. Li, S. H. Chan, J. Zhao, *ACS Appl. Mater. Interfaces* **2012**, 4, 2387.
- [9] M. C. Hsiao, S. H. Liao, Y. F. Lin, C. A. Wang, N. W. Pu, H. M. Tsai, C. C. M. Ma, *Nanoscale* **2011**, 3, 1516.
- [10] S. Stankovich, D. A. Dikin, G. H. Dommett, K. M. Kohlhaas, E. J. Zimney, E. A. Stach, R. D. Piner, S. T. Nguyen, R. S. Ruoff, *Nature* **2006**, 442, 282.
- [11] A. N. Vereshchagin, M. N. Elinson, Y. E. Anisina, F. V. Ryzhkov, A. S. Goloveshkin, R. A. Novikov, M. P. Egorov, *J. Mol. Struct.* **2017**, 1146, 766.
- [12] M. Baghayeri, H. Alinezhad, M. Tarahomi, M. Fayazi, M. Ghanei-Motlagh, B. Maleki, *Appl. Surf. Sci.* **2019**, 78, 87.
- [13] J. U. Lee, W. Lee, S. S. Yoon, J. Kim, J. H. Byun, *Appl. Surf. Sci.* **2014**, 315, 73.
- [14] X. -J. Tu, W. Fan, W. -J. Hao, B. Jiang, S. -J. Tu, *ACS Comb. Sci.* **2014**, 16, 647.
- [15] I. Muegge, *Med. Res. Rev.* **2003**, 23, 302.
- [16] L. J. Nunez-Vergara, J. A. Squella, P. A. Navarrete-Encina, E. Vicente-Garcia, S. Preciado, R. Lavilla, *Curr. Med. Chem.* **2011**, 18, 4761.
- [17] K. Sureshkumar, V. Maheshwaran, T. D. Rao, K. Themmila, M. Ponnuswamy, S. Kadhirvel, S. Dhandayutham, *J. Mol. Struct.* **2017**, 1146, 314.
- [18] A. N. Vereshchagin, M. N. Elinson, Y. E. Anisina, F. V. Ryzhkov, R. A. Novikov, M. P. Egorov, *ChemistrySelect* **2017**, 2, 4593.
- [19] A. Shaabani, F. Hajishaabanha, H. Mofakham, A. Maleki, *Mol. Diversity* **2010**, 14, 179.
- [20] M. N. Elinson, A. N. Vereshchagin, Y. E. Anisina, M. P. Egorov, *Polycycl. Aromat. Comp.* **2017**, 8, 1.
- [21] Z. Karamshahi, R. Ghorbani-Vaghei, N. Sarmast, *Mater. Sci. Eng. C* **2019**, 97, 45.
- [22] V. Štengl, S. Bakardjieva, T. M. Grygar, J. Bludská, M. Kormunda, *Chem. Cent. J.* **2013**, 7, 41.
- [23] S. N. Alam, N. Sharma, L. Kumar, *Graphene* **2017**, 6, 1.
- [24] J. Safaei-Ghommi, M. Tavazo, M. R. Vakili, H. Shahbazi-Alavi, *J. Sulfur Chem.* **2017**, 38, 236.
- [25] P. Kour, A. Kumar, V. K. Rai, *C. R. Chim.* **2017**, 20, 140.
- [26] M. A. Ghasemzadeh, M. H. Abdollahi-Basir, M. Babaei, *Green Chem. Lett. Rev.* **2015**, 8, 40.
- [27] R. Ghorbani-Vaghei, N. Sarmast, F. Rahmatpour, *C. R. Chim.* **2018**, 21, 644.
- [28] H. Sanati, Z. Karamshahi, R. Ghorbani-Vaghei, *Res Chem Intermediat.* **2019**, 45, 709.
- [29] A. Cohen, Y. Yang, Q. L. Yan, A. Shlomovich, N. Petrutik, L. Burstein, S. P. Pang, M. Gozin, *Chem. Mater.* **2016**, 28, 6118.
- [30] A. K. Mageed, D. Radiah, A. Salmiaton, S. Izhar, M. A. A. Razak, H. M. Yusoff, F. M. Yasin, S. Kamarudin, *Int. J. Appl. Chem.* **2016**, 12, 104.
- [31] A. Khalafi-Nezhad, S. Mohammadi, *RSC Adv.* **2013**, 3, 4362.

SUPPORTING INFORMATION

Additional supporting information may be found online in the Supporting Information section at the end of this article.

How to cite this article: Karamshahi Z, Ghorbani-Vaghei R, Keypour H, Rezaei MT. Highly efficient synthesis of chromeno[2,3-*b*]pyridine using Graphene-Oxide/*N¹,N³-bis* (pyridin-2-ylmethyl)propane-1,3-diamine-Copper nanocomposites as a novel catalyst. *Appl. Organomet. Chem.* 2020;e5737. <https://doi.org/10.1002/aoc.5737>